horticulturae

MDPI

Article

Genome-Wide Identification, Cloning and Expression Profile of RanBP2-Type Zinc Finger Protein Genes in Tomato

Yanna Gao [1,†], Ning Li [1,†], Jiaojiao Ruan [1], Ying Li [1], Xiaoli Liao [2] and Changxian Yang [2,*]

[1] College of Horticulture, Henan Agricultural University, Zhengzhou 450002, China
[2] Key Laboratory of Horticultural Plant Biology (MOE), Huazhong Agricultural University, Wuhan 430070, China
* Correspondence: yangcx0915@mail.hzau.edu.cn
† These authors contributed equally to this work.

Abstract: The RanBP2-type zinc finger (RBZ) protein genes, which are well-characterized in animals, are involved in the regulation of mRNA processing. Although they are diversely distributed in plants, their functions still remain largely unknown. In this study, we performed a comprehensive bioinformatic analysis of 22 *RBZ* genes in tomato. The gene structure analysis revealed that the *SlRBZ* genes have 2 to 17 exons. SlRBZ proteins contain typical conserved domains, including Motif 1 or Motif 2, or a combination of Motif 9 and Motif 4. Two paralogous pairs were identified in the tomato. Segmental duplication possibly contributed to the expansion of the *SlRBZ* genes in tomato. Interestingly, the *SlRBZ15* gene generated four products, yielded by alternative splicing. A cis-regulatory element analysis revealed that *SlRBZ* genes might be involved in the complex regulatory networks during plant growth and development. The expression profiles of the *SlRBZ* genes were analyzed in different tissues using eight phytohormones and four abiotic stress treatments based on RNA sequencing data and qRT-PCR verification. The results showed that each gene responded differently to more than one phytohormone or abiotic stress type. This research provides a foundation for future functional research on *SlRBZ* genes in tomato.

Keywords: tomato; *SlRBZ*; expression profile; phytohormones; abiotic stress

Citation: Gao, Y.; Li, N.; Ruan, J.; Li, Y.; Liao, X.; Yang, C. Genome-Wide Identification, Cloning and Expression Profile of RanBP2-Type Zinc Finger Protein Genes in Tomato. *Horticulturae* **2022**, *8*, 985. https://doi.org/10.3390/horticulturae8110985

Academic Editor: Nakao Kubo

Received: 19 September 2022
Accepted: 20 October 2022
Published: 23 October 2022

1. Introduction

The zinc finger protein superfamily comprises several subfamilies that are characterized by various structural and functional differences. Earlier studies showed that zinc finger proteins participate in a variety of biological processes, such as plant growth and development, as well as the plant's adaptation to stress and hormone responses [1]. The zinc finger (Znf) domain, which has been identified in eukaryotes, is the most well-known DNA binding domain in numerous transcription factors. One zinc finger family without the classic DNA binding function is the *RBZ* family, named after Ran Binding Protein 2 in humans [2]. The RanBP2 Znf domain (PFAM00641, IPR001876), with the conserved sequence pattern W-X-C-X(2,4)-C-X(3)-N-X(6)-C-X(2)-C, represents a new superfamily of C2C2-type zinc finger motifs. Although most members of this superfamily contain one copy of the RanBP2 Znf domain, some consist of several RanBP2 Znf domains [3].

Several human RBZ proteins, including ZRANB2, EWS, TLS/FUS, RBP56, RBM5, RBM10, and TEX13A, can bind to the cis-element GGU that is usually involved in regulation of mRNA processing in humans [4]. Previous studies have reported that *RBZ* genes participate in the differentiation and development of several organs and tissues, including seed maturation, follower development and chlorophyll biosynthesis in plants [5–8]. For example, the *GhRBZ* gene, expressed in different developmental stages of cotton glands, may play an important role in the development of the cotton gland [9]. A total of 24 *RBZ* genes have been identified in *Arabidopsis thaliana* [10]. *TATA-binding-protein-associated factor 15b* suppresses flowering by repressing the transcription elongation of *flowering locus C* [5].

Histone Deacetylase 15 (HDA15) represses chlorophyll biosynthesis in the dark, mediated by *PIF3* [7]. The suppressor of *ABSCISIC ACID-INSENSITIVE (ABI)3–5* regulates seed maturation by preventing the splicing of introns in *ABI3* [8]. There are four organelle-zinc-finger (OZ)-editing factors in *Arabidopsis*, including *OZ1* (two RanBP2 Znf domains), *OZ2* (two RanBP2 Znf domains), *OZ3* (three RanBP2 Znf domains), and *OZ4* (four RanBP2 Znf domains). Two of the OZ proteins function as key proteins in RNA processing in their respective organelles, and the remaining two are present in plastids or mitochondria [11]. *OZ1*, a key chloroplast RNA-editing factor, plays an important role in chloroplast development and germination rates in *Arabidopsis* [11]. The *oz2* null mutant presents an embryo-lethal phenotype [12]. The null mutant can be rescued by expressing the wild-type *OZ2* under the control of the seed-specific *ABI3* promoter. Recent results showed that *OZ2* is a mitochondrial splicing factor rather than an editing factor [13].

Several RBZ genes are reportedly involved in signaling pathways and biotic stimuli, including ABA, gibberellin (GA), and heat shock in plants [6,14–16]. *MYB96* induces the expression of *HDA15* and, subsequently, inhibits the expression of abscisic-acid (ABA)-signaling genes [15]. HDA15 interacts with HFR1 to repress warm-temperature responses [16]. Stress-associated RNA binding protein 1, containing three RanBP2 Znf domains without other known motifs, acts as a post-transcriptional regulatory protein. Stress-associated RNA binding protein 1 regulates the ABA signaling pathway by binding to the 3′ UTR AUUUA sequences of *ABI2*. In addition, it has been determined that rhomboid-like (RBL) protein 10 may be upregulated in response to heat shock [14].

Tomato (*Solanum lycopersicum*) is an economically important horticultural crop worldwide due to its good flavor and high nutrient value. Moreover, it is a fleshy fruit and model plant that is suitable for genetic and genomic studies. Research on the gene functions and breeding of tomato has accelerated following the sequencing, resequencing and pan-genomic analysis of wild and cultivated tomatoes [17–20]. To date, only one SlRBZ gene (*SlRBZ6*) in tomato has been characterized. *SlRBZ6* is a constitutive gene with four RanBP2 Znf domains, which may inhibit the biosynthesis of chlorophyll, carotenoids and gibberellin by blocking chloroplast development [6]. However, the characteristics and biological functions of the other majority of *SlRBZ* genes in tomato remain unknown.

In this study, we performed the genomic-wide identification and bioinformatic analysis of the *SlRBZ* gene family of tomato. A total of 22 *SlRBZ* genes were identified and isolated from the tomato. The gene structures, replication events, phylogeny, conserved motifs and cis-regulatory elements of the promoters of all the putative *SlRBZ* genes were analyzed. Moreover, we investigated the expression profiles of the genes only possessing RanBP2 Znf domains in different tissues using eight phytohormones and four abiotic stresses treatments by real-time quantitative PCR (qRT-PCR). The study provides a useful reference for the functional characterization of *SlRBZ* members in the tomato developmental processes.

2. Materials and Methods

2.1. Plant Growth Conditions and Hormone and Stress Treatments

Solanum lycopersicum L. 'Ailsa Craig' tomatoes were used as the research materials. The seeds were germinated and grown in a greenhouse (120 µmol photons/m2s, 16/8 h light/dark regimen, 25 ± 2 °C, and 60% relative humidity). The transcription levels of SlRBZ genes in one-month-old seedlings were analyzed after being subjected to several abiotic stresses and plant hormone treatments. For the phytohormone treatments, the seedlings were sprayed with solutions containing 100 µM salicylic acid (SA), 100 µM indole-3-acetic acid (IAA), 100 µM ABA, 100 µM 4-(indolyl)-butyric acid (IBA), 100 µM 6-benzylaminopurine (6-BA), 100 µM jasmonic acid (JA), 100 µM Gibberellin A3 (GA) and 1% (v/v) ethephon (ETH). A mock treatment was sprayed with water as the control. Seedling shoots were collected after 0.25, 0.5, 1, 3, 6, 9, 12, 24 and 36 h of treatment. Cold, heat, and salt stresses were applied, as we previously described [21]. Drought stress was applied using the method described in Lu et al. (2012) [22]. The samples were collected after 0.5, 1, 3, 6, 9, 12 and 24 h of treatment. Different tissues from adult plants were harvested as

we described previously [21]. All collected samples were frozen in liquid-N2 and stored at −80 °C in an ultralow-temperature refrigerator until further use.

2.2. The qRT-PCR

Total RNA was extracted using TRIzol reagent (Invitrogen, Waltham, MA, USA). The genome DNA was removed with DNase I (Takara). The cDNA was synthesized using the Transcriptor High-Fidelity cDNA Synthesis Kit (Roche). Primer 3.0 was used to design primers (Table S1). The experiment was conducted using the following parameters: a melting temperature of 60–62 °C, primer length of 23 ± 2 bp, GC content of 40–60% and product size of 80–200 bp. *Actin* was used as an internal reference for normalization. The qRT-PCR was performed using an optical 96-well plate with a LightCycler 480 system (Roche Diagnostics, Basel, Switzerland), according to the method described by Gao et al. (2015) [21]. The $2^{-\triangle\triangle Ct}$ method was used to calculate the relative expression levels of these genes [23].

2.3. Identification and Cloning of SlRBZ Genes

The consensus pattern of the RanBP2 Znf domain (PFAM00641, IPR001876) is W-X-C-X (2, 4)-C-X (3)-N-X (6)-C-X (2)-C (3). The HMMER 3.0 program was employed to search for proteins with a RanBP2 Znf domain in the tomato database. The conserved domain BLASTP searches were also performed using the tomato amino acid sequences of SlRBZ6 in the SOL Genomics Network ($E < 10^{-5}$). To confirm the results, protein sequences of the entire candidate genes were further analyzed for the presence of RanBP2 Znf domains using the online Conserved Domain Database of NCBI (https://www.ncbi.nlm.nih.gov/cdd, accessed on 20 October 2022) and SMART (http://smart.embl-heidelberg.de/, accessed on 20 October 2022). The nucleotide and amino acid sequences of the predicted *SlRBZ* genes were downloaded (File S1). ProtParam (https://web.expasy.org/protparam/, accessed on 20 October 2022) was used to calculate the basic physical and chemical characteristics (theoretical isoelectric point (PI), molecular weight (MW), etc.) of the tomato *SlRBZ* proteins. Primers (Table S1) were designed using Primer 5.0 version. Coding sequences of the SlRBZ genes from the tomato cultivar Ailsa Craig were amplified by PCR using Phanta® Super-Fidelity DNA Polymerase. The PCR products were purified and ligated to a pEasy-Blunt vector (TransGen Biotech, Beijing, China) for sequencing.

2.4. Gene Structure, Conserved Motifs and Cis-Regulatory Elements of SlRBZ Genes

To predict the exon–intron structure of the *SlRBZ* genes, a comparison between the genomic sequences and their full-length cDNA sequences was performed using the GSDS 2.0 website [24]. MEME online software was used to investigate the conserved motifs encoded by each *SlRBZ* gene [25]. The parameters were set as follows: zero or one occurrence per sequence, a motif width of 2–300, and a maximum number of 15 identified motifs. The other parameters had the default settings. The 2000 bp genomic sequences upstream of the transcription start site (ATG) of each *SlRBZ*-coding sequence were obtained from the tomato database. The PlantCARE online database was employed to analyze the putative cis-regulatory elements in the promoter regions of the *SlRBZ* genes [26].

2.5. Phylogenetic Tree and Duplication Event of SlRBZ Genes

The information regarding the RBZ proteins in *Arabidopsis* was obtained from Gipson et al. (2020) [10]. The RBZ protein sequences obtained from *Arabidopsis* and tomato for the phylogenetic analysis were separately obtained from TAIR (https://www.arabidopsis.org/, accessed on 20 October 2022) and the SGN database. The phylogenetic tree was constructed to show the phylogenetic relationships between the *RBZ* genes by the neighbor-joining method and maximum-likelihood method using the MEGA 7 software. A downloaded version of the MapChart tool was used to obtain the chromosomal location of the SlRBZ genes. To calculate the duplication event of the *SlRBZ* genes, the nonsynonymous substitution rates (Ka) and the synonymous rates (Ks) were calculated using KaKs_Calculator [27,28].

Calculated as T = Ks/2λ, the clock-like rate (λ) for the tomato was 1.5×10^{-8} substitutions/synonymous site/year [27].

2.6. RNA Sequencing Data Analysis

The data obtained from the transcriptomic analysis of various tissues in the tomato cultivar variety Heinz 1706 and the wild variety *Solanum pimpinellifolium* LA1589 were downloaded from the TFGD website (http://ted.bti.cornell.edu, accessed on 20 October 2022). The transcriptome data (raw data) of tomatoes under different abiotic stresses were also downloaded from the NCBI database, including cold (PRJEB14805), heat (PRJNA635375), drought (PRJNA635375) and salt (PRJNA624032) stress, and then reanalyzed. Clean data were obtained by removing the reads containing an adapter or ploy-N, as well as those of a low quality, and then were aligned with the reference genome (https://solgenomics.net/ftp/genomes/Solanum_lycopersicum/annotation/ITAG 2.4_release/, accessed on 20 October 2022) using Hisat2. FeatureCounts was used to count the read numbers mapped to each gene. Subsequently, TBtools was employed to calculate the fragments per kilobase of the exon model per million mapped fragments (FPKM) of each gene and create a heatmap [29].

3. Results

3.1. Identification and Isolation of the SlRBZ Genes in Tomato

Two methods were used to identify the members of the *SlRBZ* gene family in tomato. The first was to perform a BLAST search against the tomato genome using the SlRBZ6 sequences as queries. The second was to employ the consensus RanBP2 Znf domain sequences in the HMMER 3.0 program. Finally, 22 predicted *SlRBZ* genes were identified in the tomato genome. A detailed physicochemical analysis of the putative SlRBZ proteins revealed that the amino acid length and predicted MW ranged widely from 142 (aa)/15.45 kDa (*SlRBZ19*) to 1011 (aa)/111.53 kDa (*SlRBZ15*). The PI varied from 5.21 (*SlRBZ16*) to 10.87 (*SlRBZ11*). *SlRBZ19* was the minimum and *SlRBZ15* was the maximum member of the subfamily, respectively. It was found that two SlRBZ proteins, SlRBZ10 and SlRBZ12, were hydrophobic due to their positive GRAVY values, while the others were hydrophilic. The number of RanBP2 Znf domains ranged from one to four. More detailed information about the 22 *SlRBZ* genes is provided in Table 1. Coding sequences of the *SlRBZ* genes from the tomato Ailsa Craig were amplified and sequenced. The results are presented in File S2. All but four *SlRBZ* genes (*SlRBZ2/10/15/19*) matched the reference sequences. The introns of the *SlRBZ2* and *SlRBZ19* were not cleaved. The CDS length of *SlRBZ10* was 146 bp shorter than the reference sequences. Interestingly, *SlRBZ15* contained four isoforms in Ailsa Craig (Figure S1). Examining the number and sequence differences of the RanBP2 Znf domains can provide insight into their functions in tomato. A single RanBP2 Znf domain sequence was extracted from the UniProt sequence to construct an evolutionary tree using MEGA 7 (Figure S2). We observed that the Znfs within the clade I *SlRBZ* genes in the furthest C-terminal position were grouped together (Figure S2).

Table 1. Description of *SlRBZ* genes in tomato.

Gene	Annotated CDS	Gene Start (bp)	Gene End (bp)	Strand	the Number of RBZ Domains	Exon	ORF *	CDS *	AA *	PIS *	MW *	GRAVY	Domains
SlRBZ1	Solyc01g005650	455379	456988	−1	1	2	1610	1569	523	5.36	61478.64	−0.709	RBZ, IBR domain
SlRBZ2	Solyc01g044350	43255687	43259371	1	2	2	969	894	298	9.12	31513.46	−0.432	RBZ
SlRBZ3	Solyc01g057780	63862862	63868831	−1	2	5	5564	2625	875	6.99	97971.39	−0.723	RBZ
SlRBZ4	Solyc01g099230	89530334	89535887	1	2	5	5233	2352	784	6.66	89729.05	−1.11	RBZ, MSCRAMM_SdrC super family
SlRBZ5	Solyc02g032870	29438970	29441887	1	2	4	2707	1419	473	7.97	52898.98	−0.351	RBZ, TDP2
SlRBZ6	Solyc03g033560	5104384	5111275	−1	4	7	6510	996	332	9.01	36450.1	−0.63	RBZ
SlRBZ7	Solyc03g118680	67538264	67542652	−1	3	7	3994	1224	408	8.94	46033.82	−0.555	RBZ
SlRBZ8	Solyc03g119730	68283528	68292067	1	1	17	8326	1833	611	5.34	66410.65	−0.274	RBZ, HDAC_classII
SlRBZ9	Solyc05g015500	10760271	10764983	1	3	10	4350	858	286	9.14	30923.51	−0.859	RBZ
SlRBZ10	Solyc05g016380	16034731	16038070	1	1	3	3078	1116	372	8.46	42409.01	0.156	RBZ
SlRBZ11	Solyc05g018340	20573843	20579911	1	1	3	5800	1056	352	10.87	39607.39	−1.519	RBZ
SlRBZ12	Solyc07g042930	56485757	56488391	1	1	2	2125	996	332	9.82	37398.51	0.057	RBZ, Rhomboid
SlRBZ13	Solyc08g014510	4645215	4647952	−1	3	6	2452	1443	481	8.46	55095.32	−0.756	RBZ
SlRBZ14	Solyc08g067180	56155346	56156822	−1	3	3	878	513	171	8.71	18130.78	−0.782	RBZ
SlRBZ15	Solyc08g077310	61209403	61219976	1	1	16	10300	3033	1011	7.96	111526.92	−0.983	RBZ, RRM, OCRE domain, G_patch
SlRBZ16	Solyc11g008580	2764823	2775320	−1	1	15	10498	1776	592	5.21	66955.47	−0.659	RBZ, Ring finger
SlRBZ17	Solyc11g040050	40024447	40028245	1	2	7	3799	1170	390	8.62	43070.15	−1.155	RBZ, RRM_SARFH
SlRBZ18	Solyc12g006590	1079645	1080287	1	3	3	643	438	146	8.20	16061.15	−0.537	RBZ
SlRBZ19	Solyc12g006600	1083786	1084309	1	3	2	524	426	142	8.4	15446.45	−0.472	RBZ
SlRBZ20	Solyc12g011060	3931559	3932709	1	3	3	1151	498	166	8.61	18535.23	−0.41	RBZ
SlRBZ21	Solyc12g015660	5655855	5659081	−1	2	4	3227	1245	415	8.7	45811.89	−0.626	RBZ, WLM domain
SlRBZ22	Solyc12g036410	52193551	52201012	−1	2	8	7462	1803	601	8.59	65495.48	−0.168	RBZ, translation elongation factor EF-1a (GTPase)

* ORF, length of open reading frame (number of nucleotides); CDS, length of CDS; AA, protein length (number of amino acid); PIS, theoretical isoelectric point; MW, molecular weight, KDa.

3.2. Multiple Sequence Alignments and Gene Structure of SlRBZ Genes

Multiple sequence alignments were performed to examine the features of the 22 *SlRBZ* genes. The results indicated that the sequence similarity among the *SlRBZ* genes ranged widely from 30.27% to 85.46% at the nucleotide level and from 0% to 87.23% at the amino acid level (Table S2). A neighbor-joining phylogenetic tree was constructed to investigate the evolutionary relationships between the *SlRBZ* members (Figure 1A). The 22 *SlRBZ* genes were divided into three clades: I, II and III. The formation of paralogous gene pairs (*SlRBZ10/SlRBZ12* and *SlRBZ1/SlRBZ16*) had a strong bootstrap support (100%). The homology at the nucleotide level and amino acid level was 72.08% and 43.36%, and 60.06% and 49%, respectively (Table S2). The GSDS online server was employed to analyze the intron/exon structures of the SlRBZ genes. The exon number ranged from 2 to 17 (Table 1). Of the 22 *SlRBZ* genes, *SlRBZ6/7/17* had 7 exons; *SlRBZ3/4* had 5 exons; *SlRBZ5/21* had 4 exons; *SlRBZ10/11/14/18/20* had 3 exons; *SlRBZ1/2/12/19* had 2 exons; and *SlRBZ8/9/13/15/16/22* had 17, 10, 6, 16, 15 and 8 exons, respectively.

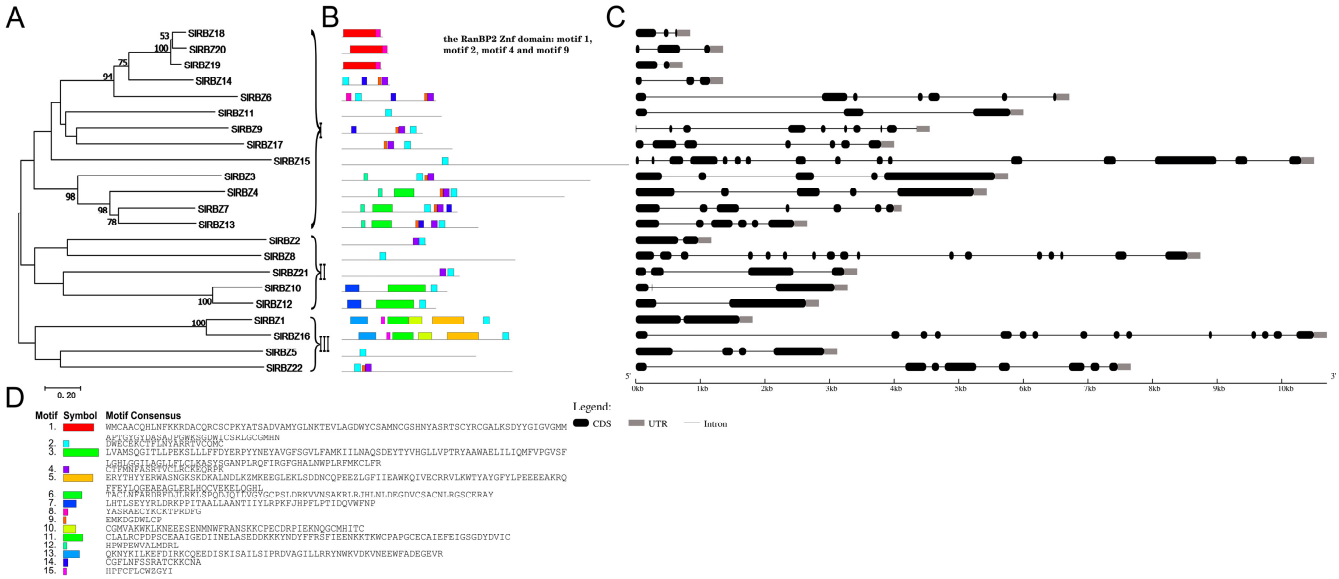

Figure 1. Phylogenetic tree (**A**), conserved motif distribution (**B**) and sequences (**D**), and gene structure (**C**) of the *SlRBZ* genes. Motif 1 or Motif 2, or a combination of Motifs 9 and 4, represent the typical RanBP2 Znf domain.

3.3. Conserved Motif Identification of SlRBZ Proteins

The MEME web server was used to predict the conserved motifs of the 22 deduced SlRBZ protein sequences. In total, we identified 15 distinct motifs (Figure 1B,D). The closest members in the phylogenetic tree, including two homologous gene pairs, always shared a common motif composition, which suggested an evolutionarily conserved and functional similarity within the same family. Meanwhile, some special motifs with unknown functions were identified. Motifs 1, 2, 9 and 4 fully matched the typical RanBP2 Znf domain of the *SlRBZ* genes based on our analyses of the Pfam and SMART databases. All these SlRBZ proteins contained Motifs 1 or Motif 2, or a combination of Motifs 9 and 4. Other motifs exhibited uniqueness in terms of some proteins, such as Motif 6 in *SlRBZ4*, *SlRBZ7* and *SlRBZ13*; Motifs 7 and 3 in *SlRBZ10* and *SlRBZ12*; and Motifs 5, 10, 11, 13 and 15 in *SlRBZ1* and *SlRBZ16*. The differing compositions of the conserved motifs may be responsible for their functional diversity.

3.4. Evolutionary Relationships and Gene Duplication of the SlRBZ Family Members

To investigate the evolutionary relationships between *RBZ* genes from different plant species, a maximum-likelihood phylogenetic tree was constructed based on the alignment of 46 *RBZ* amino acid sequences from *Arabidopsis* and tomato (Figure 2). Most of the *SlRBZ* genes, including two paralogous gene pairs (*SlRBZ10/SlRBZ12* and *SlRBZ1/SlRBZ16*), were separated by the *Arabidopsis RBZ* genes. This indicates that the genes originated before the split between tomato and *Arabidopsis*. The *SlRBZ18/19/20* genes were clustered around each other and were not separated by *Arabidopsis* genes. A similar situation occurred in four of the *ARI* genes in *Arabidopsis*. The result indicated that the genes possibly emerged after the radiation of *Arabidopsis* and tomato.

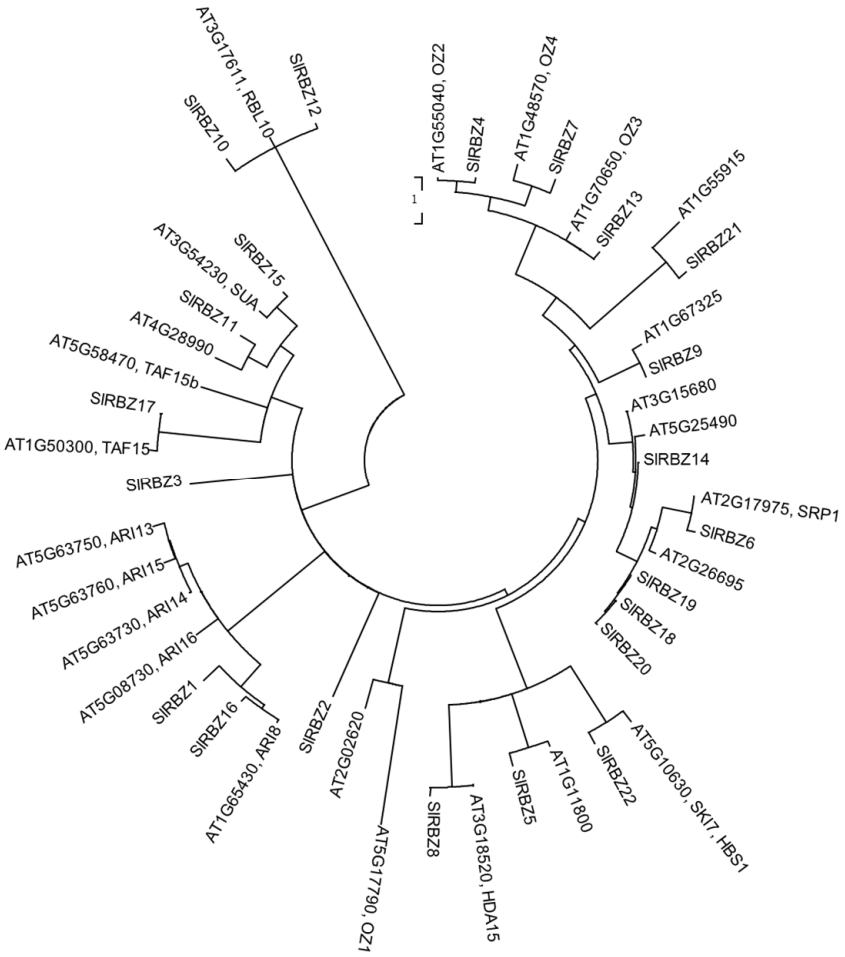

Figure 2. Phylogenetic tree of 46 *RBZ* genes from tomato and *Arabidopsis*.

The *SlRBZ* genes were unevenly distributed on 8 of the 12 tomato chromosomes (Figure 3). The number of *SlRBZ* genes appearing on each chromosome had a wide range. There were five *SlRBZ* genes on Chromosome 12 and four *SlRBZ* genes on Chromosome 1. Three *SlRBZ* genes were located on Chromosomes 3, 5 and 8, respectively, while there were two on Chromosome 11 and one on Chromosomes 2 and 7, respectively. Two gene pairs (*SlRBZ1/16* and *SlRBZ10/12*) dispersed in the genome were identified as being involved in segmental duplication events. This trend suggests that segmental duplication, rather than tandem duplication, contributes to the expansion of the *SlRBZ* genes in tomato.

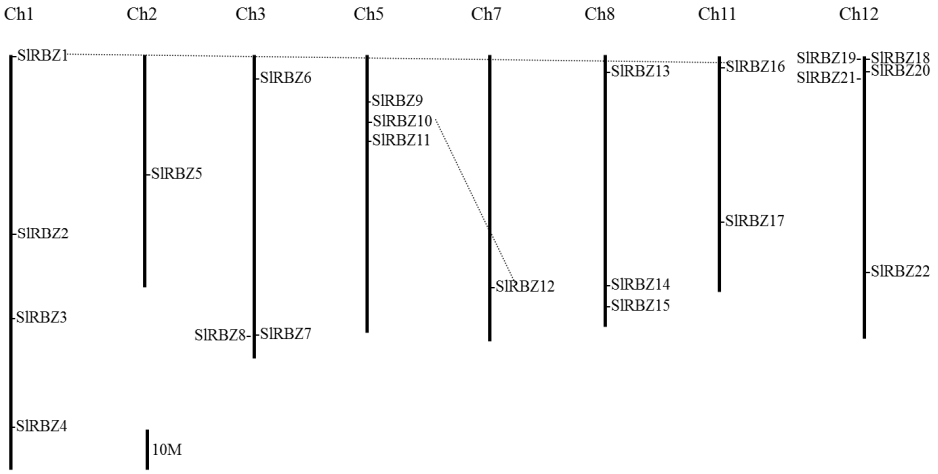

Figure 3. Chromosomal location of *SlRBZ* genes. The gene pairs are linked by dashed lines.

To assess the kinds of selection pressures among the duplicated *SlRBZ* genes, KaKs_Calculator was used to calculate the nonsynonymous (Ka) and synonymous substitutions (Ks) of the *SlRBZ* gene pairs (Table 2). The higher the Ks value is, the later the duplication events occurred. In this study, the Ka/Ks value for *SlRBZ1/16* was 0.17 (<1), indicating that the gene pairs developed through purifying selection in the tomato. However, the Ka/Ks value for *SlRBZ10/12* was 3.00 (>1), meaning that the gene pair developed through positive selection. The analysis of the dates of the duplication blocks showed that the duplication events of the *SlRBZ* genes were dated between approx. 31.60 and 69.83 million years ago (Mya), indicating that the *SlRBZ* genes expanded after the tomato/*Arabidopsis* division (~90 Mya).

Table 2. Duplicated genes and the dates of the duplication blocks of *SlRBZ* genes.

Gene1	Gene2	Ks	Ka	Ka/Ks	Date (Mya)
SlRBZ1	SlRBZ16	0.95	2.84	3	31.6
SlRBZ10	SlRBZ12	2.09	0.36	0.17	69.83

3.5. Cis-Regulatory Elements in the Promoter Regions of SlRBZ Genes

It is apparent that cis-elements play an important role in transcription control. The level of gene expression is largely dependent upon the regulation of cis-elements in different organisms. Therefore, cis-elements must be analyzed in order to predict their biological functions. Genomic sequences found 2 kb upstream of the 5′ UTR of SlRBZ genes were queried in the PlantCARE database to search for putative cis-elements. The results showed that 94 putative cis-elements were present in the promoters (Table S3). Among these, two cis-elements, CAAT-box and TATA-box, were identified in all the *SlRBZ* genes. Overall, 18 cis-elements could be found in only one gene, including the AAAC-motif in *SlRBZ22*, GC-motif in *SlRBZ11*, MSA-like motif in *SlRBZ11*, AC-I motif in *SlRBZ10* and AT-rich element in *SlRBZ18*, possibly endowing them with different biological functions. The result showed that these cis-elements can be divided into four types: stress responsiveness, light responsiveness, hormone responsiveness and plant growth and development (Figure 4).

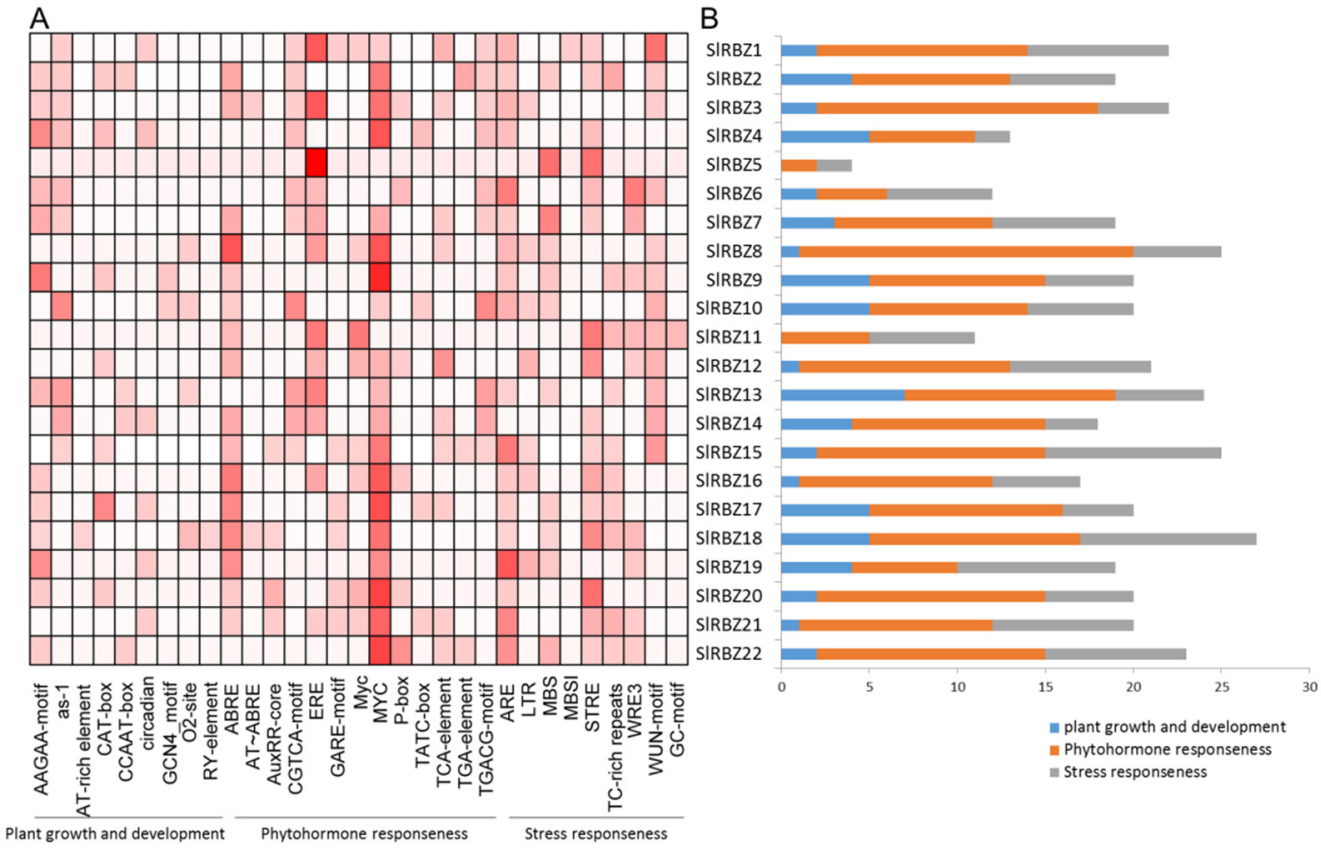

Figure 4. Information on cis-acting elements in the putative promoter regions of *SlRBZs*. (**A**) The gradient colors in the red grid indicate the numbers of cis-acting elements in the putative promoter regions of *SlRBZs*. (**B**) The *X*-axis shows the number of different types of cis-elements.

The light responsiveness group, including Box 4, the TCT-motif, G-Box and GT1-motif, were found in most of the *SlRBZ* genes. LS7, the ATCT-motif and the AAAC-motif were located in *SlRBZ9*, *SlRBZ11* and *SlRBZ22*, respectively. Additionally, we found 13 hormone responsiveness elements: ABRE (abscisic-acid (ABA)-responsive element); AT~ABRE and ERE (ethylene (ETH)-responsive elements); the CGTCA-motif and TGACG-motif (jasmonic-acid (JA)-responsive elements); TCA-element (salicylic-acid (SA)-responsive elements); GARE-motif, P-box and TATC-box (gibberellin (GA)-responsive elements); AuxRR-core and TGA-element (indole-3-acetic acid (IAA) responsiveness); and MYC and Myc, as displayed in the Supplementary Materials, Table S3. These results suggest that the transcription levels of the *SlRBZ* genes may be induced by these hormones. Furthermore, nine stress responsiveness elements were found, including MBS (drought inducibility), TC-rich repeats, MBSI and STRE (stress), ARE and GC-motif (anaerobic induction), LTR (low temperature), and WUN-motifs and WRE3 (wound responsiveness). In the plant growth and development group, some cis-elements are responsible for tissue-specific expressions, such as CAT-box in meristem cells, RY-element in the seeds, HD-Zip 1 in palisade mesophyll cells and GCN4 motif in the endosperms. These results indicate that *SlRBZ* genes might be involved in the complex regulatory networks during plant growth and development.

3.6. Tissue-Specific Expression Patterns of SlRBZ Genes

The organ/tissue-specific expression patterns of the 22 *SlRBZ* genes were investigated using bioinformatic and experimental approaches. The results are shown in a heatmap based on a publicly available RNA-seq library (Figure 5). All the *SlRBZ* genes, except for *SlRBZ1/14/18/19/20*, were constitutively expressed in all the examined tissues of Heinz (1706) (Figure 5A). Several genes in LA1589, such as *SlRBZ1/13/14/18/19/20*, were not expressed in certain tissues. The transcription levels of *SlRBZ18* were abundant in the vegetative tissues, including the hypocotyls, cotyledons, vegetative meristems and mature leaves, and were barely expressed in the reproductive tissues (Figure 5B). The *SlRBZ6/9/11/16* genes were consistently and highly expressed in Heinz (1706) and LA1589.

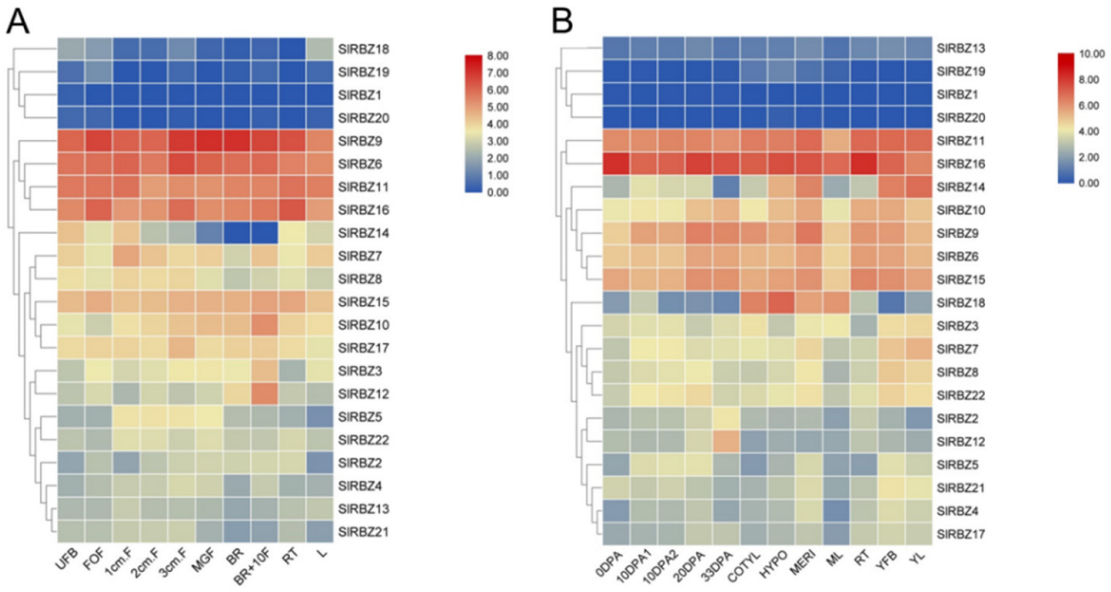

Figure 5. Heatmap of the expression profiles of *SlRBZ* genes in the cultivated tomato cultivar Heniz 1706 (**A**) and the wild species *S. pimpinellifolium* LA1589. (**B**) Fully opened flowers (FOF), unopened flower buds (UFB), 1 cm fruits (1cm.F), 2 cm fruits (2cm.F), 3 cm fruits (3cm.F), mature green fruits (MGF), breaker fruits (BR), breaker+10 fruits (BR+10F), roots (RT), leaves (L), days post-anthesis fruit (DPA), cotyledons (COTYL), hypocotyl (HYPO), vegetative meristems (MERI), mature leaves (ML), young flower buds (YFB), young leaves (YL). Dark red indicates higher expression levels, and dark blue indicates lower expression levels. Genes with similar expression profiles across various arrays are grouped on the left based on a hierarchical clustering method.

The qRT-PCR was performed to analyze the tissue expression patterns of 13 tomato *SlRBZ* genes that only have the RanBP2 Znf domain, without other known domains. All of the 13 *SlRBZ* genes were constitutively expressed in all the examined tissues (Figure 6). All the *SlRBZ* genes in tomato, except for *SlRBZ10*, had the highest relative abundance in the flowers or leaves. Nevertheless, the transcription levels of *SlRBZ10* were more abundant in the green mature stage. *SlRBZ3/9/13/18/19/20* showed similar expression patterns. The expression of the genes was highest in the leaves, followed by the red, ripe fruits, it was lowest in the immature fruits. During fruit development and ripening, the transcription levels of most of *SlRBZ* genes steadily increased; therefore, these genes may function in the late-stage development of tomatoes. In contrast, *SlRBZ10/11/14* decreased during fruit development, indicating that these three genes are involved in the early stage of the development of tomato fruits. Importantly, *SlRBZ11* was the only gene whose expression was lowest in the leaves.

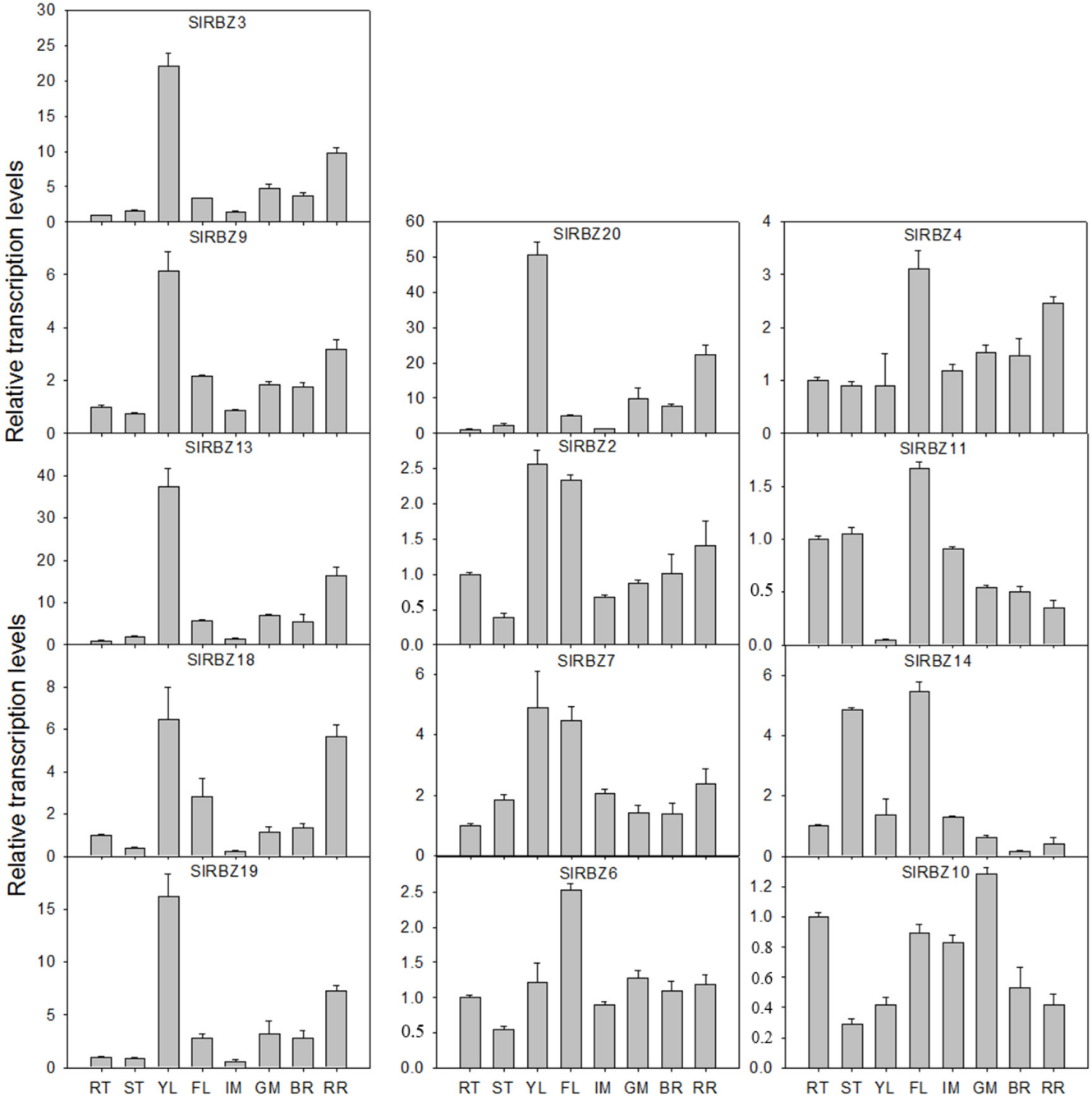

Figure 6. Expression profiles of *SlRBZ* genes in different tissues and organs. RT, root; ST, stem; YL, young leaf; FL, flower; IM, pericarp of immature fruit; GM, pericarp of mature green fruit; BR, pericarp of breaker fruit; RR, pericarp of red ripe fruit. Error bars represent standard deviations for the three replicates.

3.7. Expression Pattern of SlRBZ Genes under Different Phytohormones

Phytohormones play a crucial role in controlling the plant growth, development and response to environmental stimuli. Previous studies showed that the expression of *RBZ* genes can be induced by ABA and GA [6,14,15]. To determine whether the tomato *SlRBZ* genes can be induced by hormones, we conducted a qRT-PCR using the materials obtained after treatments with several plant hormones. *SlRBZ* genes have various responses to different plant hormones (Figure 7). *SlRBZ3/9/14/19* genes were highly induced by the ethephon treatment. The *SlRBZ9/14* expression peaked at ETH-3 h, while the *SlRBZ3/19* expression peaked at ETH-9 h. The transcription levels of these genes were 41.65 to

3061.45 times higher than those of the mock treatment. The *SlRBZ7/13* genes were induced at GA-9 h by 4.86 and 116.70 times. Some genes were induced by JA, such as *SlRBZ4/10,* which was induced by JA-9 h by 2463.80 and 148.40 times. *SlRBZ6* was also induced slightly by JA-24 h by 3.60 times. *SlRBZ2/20* was induced strongly by 6BA-12 h by 10,297.45 and 186,222.30 times. The *SlRBZ18* expression peaked at ABA-12 h after treatment by about 166.96 times. The *SlRBZ11* expression peaked at SA-12 h by approximately 6.89 times. *SlRBZ6* was not sensitive to these hormones (Figure S3).

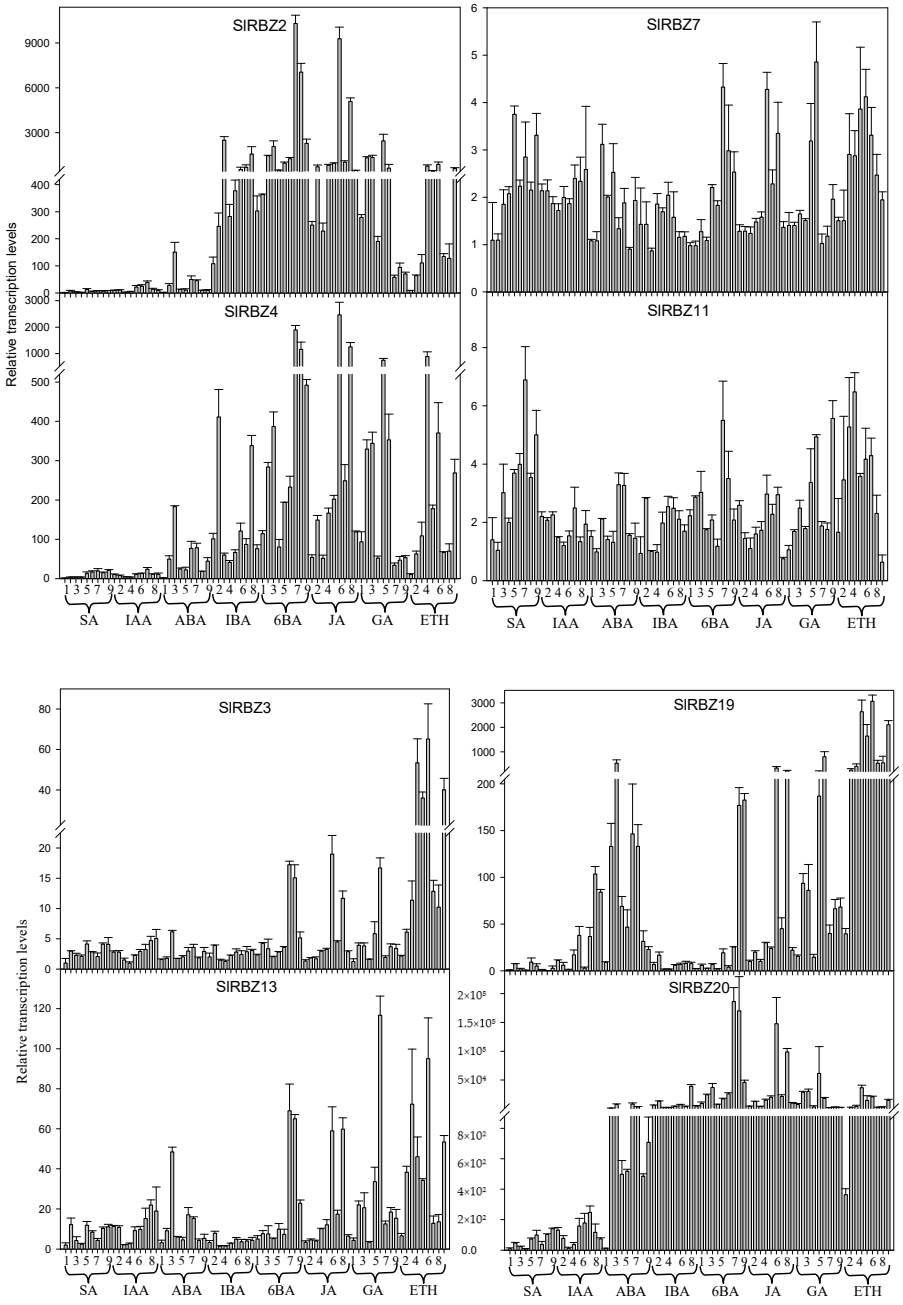

Figure 7. *Cont.*

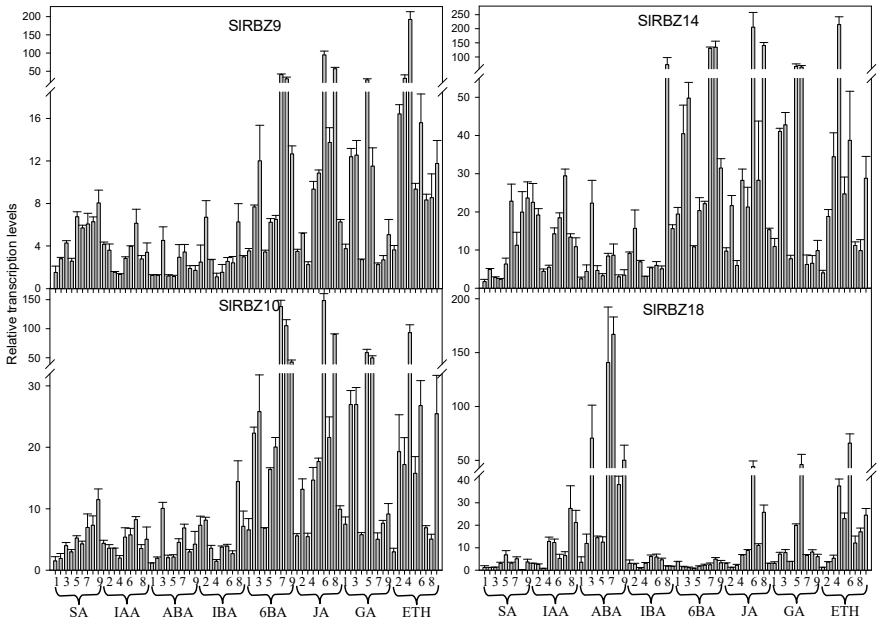

Figure 7. Expression profiles of the *SlRBZ* genes under exogenous phytohormone treatments. The numbers (1–9) below the *x*-axis represent the time course of the hormone treatment, e.g., for 1: 0.25 h; 2, 0.5 h; 3, 1 h; 4, 3 h; 5, 6 h; 6, 9 h; 7, 12 h; 8, 24 h; 9, 36 h. Here, the number is the interval, displayed for clarity. The *y*-axis represents the relative transcription levels of the *SlRBZ* genes compared to the mock, which was sprayed with water. Error bars represent standard deviations for the three replicates.

3.8. Expression Characteristics of the SlRBZ Genes under Various Abiotic Stresses

To assess the potential functions of the *SlRBZs* in response to different abiotic stresses (cold, heat, drought and salt), a transcriptome analysis, combined with a qRT-PCR assay, was employed (Figures 8 and 9). Under the chilling treatment, the expression of *SlRBZ6/9/13/15/16* genes exhibited a decreasing trend in response to the 15 °C treatment in the case of LA1777 and Moneymaker. In contrast, the other genes were insensitive to the chilling treatment. The *SlRBZ* genes exhibited three distinct patterns under heat stress. Whereas *SlRBZ3/4/7/9/17/18* showed an obvious upward trend, *SlRBZ14/15* showed an obvious downward trend. *SlRBZ16* showed a downward trend first and then an upward trend. About 50% of the *SlRBZ* genes (11 of 22) were induced by drought stress. Seven *SlRBZ* genes (*SlRBZ6/8/10/14/16/18/22*) were significantly suppressed by salt. However, the *SlRBZ2/3/4/13* genes were induced by salt at 8 h.

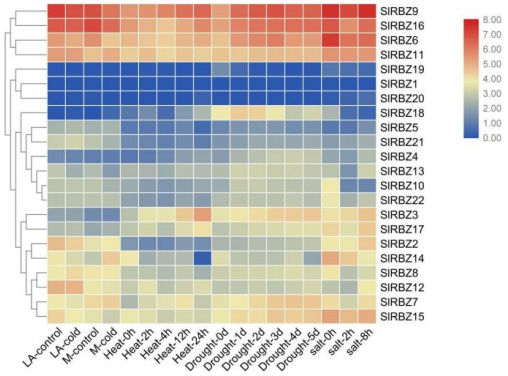

Figure 8. Expression patterns of *SlRBZ* genes under abiotic stresses based on RNA-seq. Moneymaker (M) and LA1777 (LA) were treated for 3 d at 23 °C and 15 °C. Under heat and drought conditions, the seedlings of *Solanum lycopersicum* cv M82 were kept under 42 °C and the drought treatment, respectively. In salt, the seedlings of Micro-Tom were sprayed with 200 mM NaCl.

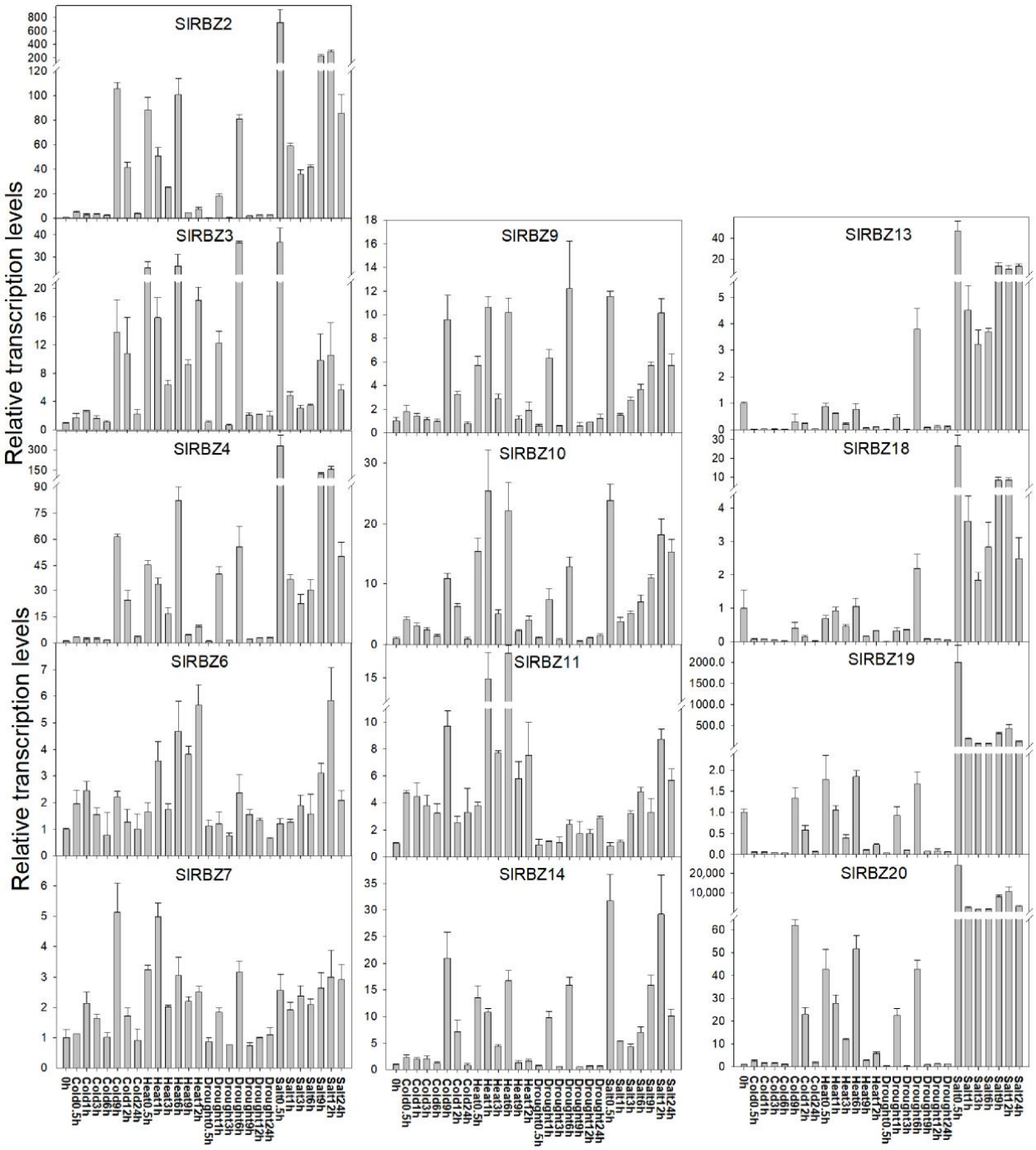

Figure 9. Expression patterns of *SlRBZ* genes under abiotic stresses by qRT-PCR. Error bars represent standard deviations for the three replicates.

The transcript profiles of 13 *SlRBZ* genes, which only have the RanBP2 Znf domain, without other known domains, were analyzed under different abiotic stresses by qRT-PCR analysis (Figure 9). All the examined *SlRBZ* genes could be induced differently by more than one abiotic stress. Most of the examined *SlRBZ* genes were strongly induced by salt, with the highest transcription levels observed at 0.5 h after treatment. Among the genes, the *SlRBZ20* expression peaked at salt-0.5 h, with an expression 2.43e4 times higher than that of the mock treatment. *SlRBZ6/15* were induced by salt at 12 h and 24 h, respectively. All the examined *SlRBZ* genes, except for *SlRBZ6/13/18/19*, were positively affected by cold, heat and drought. The *SlRBZ6* transcription levels remained unchanged under cold and

drought stress conditions. Interestingly, *SlRBZ13/18/19* were downregulated in response to cold and heat treatments, as well as drought treatment. The expression levels of *SlRBZ9* were increased by all four treatments, with the highest induction observed in response to the drought and salt treatments (approximately 12 times). The transcription level of *SlRBZ11* was highly increased at 6 h after heat stress, with an expression 18.68 times that of the mock treatment.

4. Discussion

RBZ transcription factors are common in animals and plants. This type of transcription factor was first discovered in the nuclear export protein RanBP2 and is involved in mRNA processing in humans [30,31]. However, it has not yet been widely characterized in plants. Similar to other zinc finger proteins, *RBZ* transcription factors are highly conserved between species. The number of *RBZ* family members in tomato is similar to that in *Arabidopsis.* It has been reported that the expansion of gene families results from gene duplication events, including segmental and tandem duplications [32]. The duplicated genes start with the same sequence and then develop different regulatory and coding regions [33]. Segmental duplication likely contributed to the expansion of the *SlRBZ* gene family.

The multiple sequence alignment results show that the sequence similarity of the *SlRBZ* genes at the nucleotide level was 30.27~85.46% and the similarity at the amino acid level was 0~87.23% based on the multiple sequence alignments. Therefore, the *SlRBZ* genes were highly complex, according to the widely varied nucleotide sequences' lengths and exon numbers. This suggests that *SlRBZ* genes may be involved in different biological processes. Accordingly, the SlRBZ proteins contain various conserved motifs based on the motif analysis using the MEME network. The examination of the number and sequence differences between the RanBP2 Znf domains can provide insight into their functions within the full-length protein. In this study, the number and sequence differences between the RanBP2 Znf domains on the *SlRBZ* genes were also examined. Our results show that the number of RanBP2 Znf domains ranges from 1 to 4, and the sequence is well conserved across its different iterations. This supports earlier studies involving *Arabidopsis* [10]. Alternative splicing is an important transcriptional regulatory mechanism and is widely found in eukaryotes. Previous studies have shown that 95% of the human genes containing multiple exons have alternative splicing [34]. There are many splicing types, including the skipped exon types, intron retention, competing 5′ splice sites, etc. Our results show that *SlRBZ2*, *SlRBZ15* and *SlRBZ19* may undergo intron retention. Similarly, alternative splicing events of the *RBZ* genes were also found in *Arabidopsis* [10]

The characterization of genes' expression patterns reveals their regulatory roles in plant growth and development. Our results show that all the examined SlRBZ genes were constitutively expressed in the eight examined tissues. *HDA15* is highly expressed in the stems throughout the life of *Arabidopsis* [35]. *AtRBL10* is expressed consistently across the plant tissues and their development, and it plays a positive role in heat shock [14]. The transcription levels of *SlRBZ10* (the orthologous gene of *AtRBL10*) were more abundant in the green mature stage and became progressively lower during fruit development, thus indicating that *SlRBZ10* plays a role in the early stage of the development of tomato fruits. Furthermore, the *SlRBZ10* expression was significantly upregulated following heat treatment in this study. This indicated that *SlRBZ10* and *AtRBZ10* may have similar functions in response to heat shock. In this study, the transcription levels of *SlRBZ6* were induced by the eight examined phytohormones by 4-fold less than the control induced by qRT-PCR. Fan et al. (2015) reported that *SlRBZ6* was induced by GA-24 h and IAA-1 h by five-fold less than the control and was not sensitive to ABA [6]. This is similar to our experimental results.

Plant hormones play important roles in various abiotic and biotic stresses during plant development [36]. Abiotic stress (including extreme temperature, high salinity and drought) is the leading cause of crop loss worldwide, resulting in average yield declines of more than 50% in most major crops. In this study, most of the *SlRBZ* genes were induced by hormones or abiotic stress, which was consistent with the prediction regarding their promoter cis-regulatory elements. For example, the expression level of *SlRBZ2/14/18/19/20* was high under the ABA treatment (Figure 7). *SlRBZ3/18/20* was induced to varying degrees by GA. *SlRBZ3/10* was induced 9 h after the cold treatment, confirming the predicted low-temperature responsiveness of the cis-regulatory elements in the promoter region (Table S3). This indicated that *SlRBZ3/10* is likely to be involved in the cold–stress response. The expression level of *SlRBZ2/7/9/10/13/18/19* was induced after the drought treatment, supporting the predicted drought responsiveness of the cis-regulatory elements in the promoter region (Table S3).

Both a transcriptome analysis and qRT-PCR assay were employed to assess the potential functions of the *SlRBZs* in response to different abiotic stresses. The transcription levels of *SlRBZ13* were suppressed by cold, *SlRBZ19* was suppressed by drought and *SlRBZ9* was induced by heat and drought in the qRT-PCR analysis (Figure 9). These results were consistent with the changes in the RNA-seq data. *SlRBZ6/20* were induced by salt at 12 h and 0.5 h in the qRT-PCR analysis (Figure 9). However, *SlRBZ6* was suppressed by salt based on the RNA-seq data. There was no obvious change in the expression of *SlRBZ20* after the salt treatment based on the RNA-seq data (Figure 8). Therefore, the results do not confirm the changes in the RNA-seq data. This difference might be caused by the different materials or different stress treatment times and methods employed.

5. Conclusions

This study undertook a comprehensive, genome-wide gene identification of the RBZ family in tomato. A total of 22 *SlRBZ* genes were identified. We analyzed the phylogeny, conserved motifs, gene structure, chromosomal location, cis-elements and expression patterns of all the *SlRBZ* genes in different tissues from tomato using bioinformatics methods. A qPCR analysis was performed to analyze the tissue expression levels of the *SlRBZ* genes in tomato to induce the expression levels under the effects of eight different hormones and four abiotic stress treatments. The results showed that most of the *SlRBZ* genes responded to at least one abiotic stress or plant hormone, thereby indicating their potential functions in such processes. In general, this research provides comprehensive information and a basis for future functional research on the *SlRBZ* genes in tomato.

Supplementary Materials: The following supporting information can be downloaded at: https://www.mdpi.com/article/10.3390/horticulturae8110985/s1, File S1. The nucleotide and amino acid sequences of 22 identified SlRBZ genes downloaded from the SOL Genomics Network. File S2. The coding sequences of 22 identified SlRBZ genes in Ailsa Craig. Figure S1. Gene structure of different transcripts of SlRBZ15. Figure S2. Phylogenetic tree of tomato RanBP2 zinc finger domains. Figure S3. Expression profiles of SlRBZ6 under exogenous phytohormone treatments. Table S1. Primers used in this study. Table S2. Multiple Sequence Alignments were carried out with the ClustalW2 web server using the nucleotide (nt)a and amino acid (aa)b sequences of the SlRBZ genes. Table S3. A total of 94 cis-elements identified using PlantCARE program in the promoter regions of the SlRBZ genes.

Author Contributions: Y.G. designed the experiments, carried out the inducing of the expression profiles, analyzed the data and drafted the manuscript. J.R. and N.L. carried out the amplification of the sequences of *SlRBZ* genes and analyzed the data. N.L. analyzed the cis-regulatory elements within the promoters and conserved motifs of the *SlRBZ* genes. X.L. and Y.L. performed the qRT-PCR for the tissue-preferential expression profiles of the *SlRBZ* genes and analyzed the data. C.Y. designed the experiments and revised the manuscript. All authors have read and agreed to the published version of the manuscript.

Funding: This work was supported by grants from the National Natural Science Foundation of China (No. 31801880). The Key Research and Development Foundation of Henan (No. 222102110407).

Institutional Review Board Statement: Not applicable.

Informed Consent Statement: Not applicable.

Data Availability Statement: Not applicable.

Conflicts of Interest: The authors declare no conflict of interest.

References

1. Laity, J.H.; Lee, B.M.; Wright, P.E. Zinc finger proteins: New insights into structural and functional diversity. *Curr. Opin. Struct. Biol.* **2001**, *11*, 39–46. [CrossRef]
2. Singh, B.B.; Patel, H.H.; Roepman, R.; Schick, D.; Ferreira, P.A. The zinc finger cluster domain of RanBP2 is a specific docking site for the nuclear export factor, Exportin-1. *J. Biol. Chem.* **1999**, *274*, 37370–37378. [CrossRef] [PubMed]
3. Lu, S.; Wang, J.; Chitsaz, F.; Derbyshire, M.K.; Geer, R.C.; Gonzales, N.R.; Gwadz, M.; Hurwitz, D.; Marchler, G.H.; Song, J.S.; et al. CDD/SPARCLE: The conserved domain database in 2020. *Nucleic. Acids Res.* **2020**, *48*, 265–268. [CrossRef] [PubMed]
4. Nguyen, C.D.; Mansfield, R.E.; Leung, W.; Vaz, P.M.; Loughlin, F.E.; Grant, R.P.; Mackay, J.P. Characterization of a Family of RanBP2-Type Zinc Fingers that Can Recognize Single-Stranded RNA. *J. Mol. Biol.* **2011**, *407*, 273–283. [CrossRef]
5. Eom, H.; Park, S.J.; Kim, M.K.; Kim, H.; Kang, H.; Lee, I. TAF15b, involved in the autonomous pathway for flowering, represses transcription of FLOWERING LOCUS C. *Plant J.* **2018**, *93*, 79–91. [CrossRef]
6. Fan, M.; Gao, S.; Ren, J.; Yang, Q.; Li, H.; Yang, C.; Ye, Z. Overexpression of SlRBZ results in chlorosis and dwarfism through impairing chlorophyll, carotenoid, and gibberellin biosynthesis in tomato. *Front. Plant Sci.* **2016**, *7*, 907. [CrossRef]
7. Liu, X.; Chen, C.Y.; Wang, K.C.; Luo, M.; Tai, R.; Yuan, L.; Zhao, M.; Yang, S.; Tian, G.; Cui, Y.; et al. Phytochrome Interacting FACTOR3 Associates with the histone deacetylase HDA15 in repression of chlorophyll biosynthesis and photosynthesis in etiolated *Arabidopsis* seedlings. *Plant Cell* **2013**, *25*, 1258–1273. [CrossRef]
8. Sugliani, M.; Brambilla, V.; Clerkx, E.J.M.; Koornneef, M.; Soppe, W.J.J. The conserved splicing factor SUA controls alternative splicing of the developmental regulator ABI3 in *Arabidopsis*. *Plant Cell* **2010**, *22*, 1936–1946. [CrossRef]
9. Chang, P.A.; Li, B.; Ni, X.M.; Xie, Y.F.; Cai, Y.F. Molecular cloning and expression analysis of a RanBP2 zinc finger protein gene in upland cotton (Gossypium hirsutum L.). *Colloids Surf. B Biointerfaces* **2007**, *55*, 153–158. [CrossRef]
10. Gipson, A.B.; Giloteaux, L.; Hanson, M.R.; Bentolila, S. Arabidopsis RanBP2-Type Zinc Finger Proteins Related to Chloroplast RNA Editing Factor OZ1. *Plants* **2020**, *9*, 307. [CrossRef]
11. Sun, T.; Shi, X.; Friso, G.; Van Wijk, K.; Bentolila, S.; Hanson, M.R. A zinc finger motif-containing protein is essential for chloroplast RNA editing. *PLOS Genet.* **2015**, *11*, e1005028. [CrossRef] [PubMed]
12. Ju, Y.; Liu, C.; Lu, W.; Zhang, Q.; Sodmergen. Arabidopsis mitochondrial protein slow embryo development is essential for embryo development. *Biochem. Biophys. Res. Commun.* **2016**, *474*, 371–376. [CrossRef] [PubMed]
13. Bentolila, S.; Gipson, A.B.; Kehl, A.J.; Hamm, L.N.; Hayes, M.L.; Michael, M.R.; Hanson, M.R. A RanBP2-type zinc finger protein functions in intron splicing in Arabidopsis mitochondria and is involved in the biogenesis of respiratory complex I. *Nucleic Acids Res.* **2021**, *49*, 3490–3506. [CrossRef] [PubMed]
14. Knopf, R.R.; Adam, Z. Rhomboid proteases in plants—Still in square one? *Physiol. Plant.* **2012**, *145*, 41–51. [CrossRef]
15. Lee, H.G.; Seo, P.J. MYB96 recruits the HDA15 protein to suppress negative regulators of ABA signaling in Arabidopsis. *Nat. Commun.* **2019**, *10*, 1713. [CrossRef]
16. Shen, Y.; Lei, T.; Cui, X.; Liu, X.; Zhou, S.; Zheng, Y.; Guérard, F.; Issakidis-Bourguet, E.; Zhou, D.X. Arabidopsis histone deacetylase HDA15 directly represses plant response to elevated ambient temperature. *Plant J.* **2019**, *100*, 991–1006. [CrossRef]
17. The Tomato Genome Consortium. The Tomato Genome Sequence Provides Insights into Fleshy Fruit Evolution. *Nature* **2012**, *485*, 635–641. [CrossRef]
18. Causse, M.; Desplat, N.; Pascual, L.; Le Paslier, M.-C.; Sauvage, C.; Bauchet, G.; Bérard, A.; Bounon, R.; Tchoumakov, M.; Brunel, D.; et al. Whole genome resequencing in tomato reveals variation associated with introgression and breeding events. *BMC Genom.* **2013**, *14*, 791. [CrossRef]
19. Lin, T.; Zhu, G.; Zhang, J.; Xu, X.; Yu, Q.; Zheng, Z.; Zhang, Z.; Lun, Y.; Li, S.; Wang, X.; et al. Genomic analyses provide insights into the history of tomato breeding. *Nat. Genet.* **2014**, *46*, 1220–1226. [CrossRef]
20. Gao, L.; Gonda, I.; Sun, H.; Ma, Q.; Bao, K.; Tieman, D.M.; Burzynski-Chang, E.A.; Fish, T.L.; Stromberg, K.A.; Sacks, G.L.; et al. The tomato pan-genome uncovers new genes and a rare allele regulating fruit flavor. *Nat Genet.* **2019**, *51*, 1044–1051. [CrossRef]
21. Gao, Y.; Gao, S.; Xiong, C.; Yu, G.; Chang, J.; Ye, Z.; Yang, C. Comprehensive analysis and expression profile of the homeodomain leucine zipper IV transcription factor family in tomato. *Plant Physiol. Bioch.* **2015**, *96*, 141–153. [CrossRef] [PubMed]
22. Lu, Y.; Ouyang, B.; Zhang, J.; Wang, T.; Lu, C.; Han, Q.; Zhao, S.; Ye, Z.; Li, H. Genomic organization, phylogenetic comparison and expression profiles of annexin gene family in tomato (*Solanum Lycopersicum*). *Gene* **2012**, *499*, 14–24. [CrossRef] [PubMed]
23. Livak, K.J.; Schmittgen, T.D. Analysis of relative gene expression data using real-time quantitative PCR and the 2(-DeltaC(T)) Method. *Methods* **2001**, *25*, 402–408. [CrossRef]

24. Hu, B.; Jin, J.; Guo, A.Y.; Zhang, H.; Luo, J.; Gao, G. GSDS 2.0: An upgraded gene feature visualization server. *Bioinformatics* **2015**, *31*, 1296–1297. [CrossRef]
25. Bailey, T.L.; Johnson, J.; Grant, C.E.; Noble, W.S. The MEME Suite. *Nucleic Acids Res.* **2015**, *43*, W39–W49. [CrossRef]
26. Lescot, M.; Déhais, P.; Thijs, G.; Marchal, K.; Moreau, Y.; Van De Peer, Y.; Rouzé, P.; Rombauts, S. PlantCARE, a database of plant cis-acting regulatory elements and a portal to tools for in silico analysis of promoter sequences. *Nucleic Acids Res.* **2002**, *30*, 325–327. [CrossRef]
27. Koch, M.A.; Haubold, B.; Mitchell-Olds, T. Comparative evolutionary analysis of chalcone synthase and alcohol dehydrogenase loci in arabidopsis, arabis, and related genera (Brassicaceae). *Mol. Biol. Evol.* **2000**, *17*, 1483–1498. [CrossRef] [PubMed]
28. Zhang, Z. KaKs_calculator 3.0: Calculating selective pressure on coding and non-coding sequences. *Genom. Proteom. Bioinform.* **2022**, *3*, S1672-0229(21)00259-X. [CrossRef]
29. Chen, C.; Chen, H.; Zhang, Y.; Thomas, H.R.; Frank, M.H.; He, Y.; Xia, R. TBtools: An integrative toolkit developed for interactive analyses of big biological data. *Mol. Plant* **2020**, *13*, 1194–1202. [CrossRef]
30. Gamsjaeger, R.; Liew, C.K.; Loughlin, F.E.; Crossley, M.; Mackay, J.P. Sticky fingers: Zinc-fingers as protein-recognition motifs. *Trends Biochem. Sci.* **2007**, *32*, 63–70. [CrossRef] [PubMed]
31. Higa, M.M.; Alam, S.L.; Sundquist, W.I.; Ullman, K.S. Molecular characterization of the Ran-binding zinc finger domain of Nup153. *J. Biol. Chem.* **2007**, *282*, 17090–17100. [CrossRef] [PubMed]
32. Cannon, S.B.; Mitra, A.; Baumgarten, A.; Young, N.D.; May, G. The roles of segmental and tandem gene duplication in the evolution of large gene families in Arabidopsis thaliana. *BMC Plant Biol.* **2004**, *4*, 10. [CrossRef] [PubMed]
33. Xu, G.; Guo, C.; Shan, H.; Kong, H. Divergence of duplicate genes in exon-intron structure. *Proc. Natl. Acad. Sci. USA* **2012**, *109*, 1187–1192. [CrossRef] [PubMed]
34. Zhang, F.; Deng, C.K.; Wang, M.; Deng, B.; Barber, R.; Huang, G. Identification of novel alternative splicing biomarkers for breast cancer with LC/MS/MS and RNA-Seq. *BMC Bioinform.* **2020**, *21*, 541. [CrossRef] [PubMed]
35. Alinsug, M.V.; Chen, F.F.; Luo, M.; Tai, R.; Jiang, L.; Wu, K. Subcellular localization of Class II HDAs in Arabidopsis thaliana: Nucleocytoplasmic shuttling of HDA15 is driven by light. *PLoS ONE* **2012**, *7*, e30846. [CrossRef]
36. Ku, Y.S.; Sintaha, M.; Cheung, M.Y.; Lam, H.M. Plant Hormone Signaling Crosstalks between Biotic and Abiotic Stress Responses. *Int. J. Mol. Sci.* **2018**, *19*, 3206. [CrossRef]